Reproductive Sciences
2016, Vol. 23(11) 1580-1592

DOI: 10.1177/1933719116648216
rs.sagepub.com
SAGE

# Nectin-3 Is Increased in the Cell Junctions of the Uterine Epithelium at Implantation

**Connie E. Poon, PhD[1,2], Romanthi J. Madawala, PhD[1,2], Samson N. Dowland, PhD[1,2], and Christopher R. Murphy, PhD, DSc[1,2]**

**Abstract**

Uterine luminal epithelial cells (UECs) undergo the plasma membrane transformation in the transition to receptivity. This involves transient alterations in the apical junctional complex (AJC) including increases to the depth and complexity of the tight junction, loss of the adherens junction, and a decrease in the number of desmosomes along the lateral cell membranes. Nectin-3 is key protein involved in the structure and function of the AJC. This study, used immunofluorescence, Western blotting, colocalization, and coimmunoprecipitation analyses, to investigate whether nectin-3 was present in the rat uterus and was regulated by hormones and the blastocyst during early pregnancy. The results showed that nectin-3 was present in UECs as 3 molecular weight protein isoforms (80 kDa, 60 kDa, and 32 kDa). At the time of fertilization (day 1 of pregnancy), nectin-3 was localized basally, but at the time of implantation, (day 6 of pregnancy) when UECs were receptive, nectin-3 increased in the cellular junctions. When UECs returned to the nonreceptive state (day 9 of pregnancy), nectin-3 redistributed back to the cell cytoplasm. This study also showed that nectin-3 localization at the cell junctions was likely to be controlled by progesterone; however, neither ovarian hormones nor the blastocyst regulated protein abundance. This study further showed that while nectin-3 localized to the tight junction at the time of implantation, it did not interact with occludin or l-afadin. These results suggest that at the time of implantation, nectin-3 may contribute to the formation of the tight junction in a protein complex independent from occludin and l-afadin.

**Keywords**

endometrium, implantation, estrogen, pregnancy, progesterone

## Introduction

The uterine luminal epithelial cells (UECs) form an intact epithelial barrier that maintains mucosal integrity and prevents invasion by the blastocyst and pathogenic agents during the nonreceptive state.[1] However, UECs undergo major alterations to transition to a receptive state to permit attachment and subsequent invasion by the blastocyst for pregnancy, largely in response to ovarian hormones, progesterone and estrogen.[2] The plasma membrane transformation describes these morphological and biochemical modifications that occur in UECs and involves major alterations to the apical junctional complex (AJC).[1]

The AJC is an important defining feature of all simple and polarized epithelia and is formed by 3 intercellular junctions, the tight junction, the adherens junction, and the desmosome.[3,4] The tight junction serves to maintain apicobasal polarization and also regulates the movement of fluid through the paracellular pathway.[5,6] The adherens junction and the desmosome serve to maintain strong intercellular adhesion that provides structural support for connection with the cellular cytoskeleton and maintains the integrity of the epithelial barrier.[4,7]

Previous ultrastructural studies of rat UECs have shown that leading up to the time of implantation, the tight junction increases in depth and complexity,[8] the adherens junction is lost,[9] and the desmosomes decrease in number.[10] Similar changes have also been documented in the uteri of other species, including mice,[11-13] pigs,[14,15] rabbits,[16-18] and humans.[19-21] These alterations permit preservation of the uterine luminal contents and loosening of the epithelial adhesions in preparation for blastocyst attachment and invasion to the underlying uterine stroma for pregnancy.[9]

Besides the ultrastructure of the AJC, many of the proteins that form the AJC have also been investigated previously in rat UECs during early pregnancy including tight junction proteins, claudin-1,[22,23] claudin-3, claudin-4,[22] and occludin[22,23];

[1] Cell and Reproductive Biology Laboratory, School of Medical Sciences (Discipline of Anatomy and Histology), The University of Sydney, Sydney, New South Wales, Australia
[2] The Bosch Institute, The University of Sydney, Sydney, New South Wales, Australia

**Corresponding Author:**
Connie E. Poon, Cell and Reproductive Biology Laboratory, School of Medical Sciences (Discipline of Anatomy and Histology), The University of Sydney, N364, F13 Anderson Stuart Building, New South Wales 2006, Australia.
Email: conniep@anatomy.usyd.edu.au

adherens junction proteins, pan-cadherin,[24] and E-cadherin[25]; and desmosome proteins, desmoglein-1 and desmoglein-2.[26] Another protein that is frequently involved in the formation of the adherens junction but that has not yet been investigated specifically in the rat uterus during early pregnancy is nectin-3.[27]

Nectin-3 (also known as PVRL3) is a $Ca^{2+}$-independent immunoglobulin (Ig)-like cellular adhesion molecule that belongs to the nectin family of proteins and structurally consists of an extracellular domain with 3 Ig-like loops, a single transmembrane domain and a cytoplasmic tail.[28] Nectin-3 has 3 splice variants that have been proposed to yield 3 protein isoforms of different molecular weights: nectin-3α (60 kDa), nectin-3β (55 kDa), and nectin-3γ (47 kDa).[27] Nectin-3 is documented to serve as an intercellular adhesion protein that is required for the formation and maintenance of adherens junctions and tight junctions in epithelial tissues.[27] Adhesion is mediated through the formation of homo-*cis*-dimers followed by hetero-*trans*-dimers with other members of the nectin family.[27]

Nectin-3 also provides a stimulatory signal that sequentially recruits E-cadherin and then claudins for the formation of the adherens junction and the tight junction, respectively.[29] Binding of the nectin-3 cytoplasmic tail to the PDZ domain of the F-actin-binding protein, afadin, further strengthens these junctions.[30] Studies involving the knockout of nectin-3 protein in the testis demonstrate the critical role that nectin-3 plays in the maintenance of the epithelial barrier.[31]

Nectin-3 has been found previously in the glandular epithelia of human endometrium.[32] This protein is also present in the mouse embryo during the early stages of development.[33] Given the role of nectin-3 in the formation and maintenance of the AJC in other epithelial tissues and its reported presence in the human endometrium, this study sought to investigate whether nectin-3 protein was present in the rat endometrium during early pregnancy when the AJC undergoes major alterations in UECs in the transition to receptivity. It was hypothesized that nectin-3 may be present at the AJC at the time of fertilization when the adherens junction is intact but may be downregulated at the time of receptivity when the adherens junction is lost. The second part of this study examined whether ovarian hormones or the blastocyst regulate the colocalization and abundance of nectin-3 protein. The final part of this study investigated whether nectin-3 colocalized and interacted with occludin and l-afadin to elucidate a role in the formation of the tight junctions and the actin cytoskeleton.

## Materials and Methods

### Pregnant Animals

Female virgin Wistar rats aged 10 to 12 weeks were used in this study. The University of Sydney Ethics Committee approved all experimental procedures. Animals were maintained under a 12-hour light–dark cycle at a temperature of 21°C and were fed and watered ad libitum. Vaginal smears were performed to stage the estrous cycle of female rats, and those in proestrus were mated with a fertile male overnight. Mating was confirmed the following morning by the presence of spermatozoa in the vaginal smear and that same day was designated day 1 of pregnancy. Pregnant rats were selected at random for sacrifice on days 1 (preimplantation), 3, 6 (implantation), 7, and 9 (postimplantation) of pregnancy and were euthanized with an intraperitoneal injection of sodium pentobarbital (10 mg/kg body weight, Nembutal; Merial Australia, Macquarie Park, NSW, Australia). The uterine horns from pregnant animals were collected for immunofluorescence (25 rats total, 5 rats per day of pregnancy), Western blotting (20 rats total, 5 rats per day of pregnancy), or immunoprecipitation (IP; 12 rats total, day 6 of pregnancy only).

### Pseudopregnant Animals

Female rats in proestrus were mated with a vasectomized male overnight to induce pseudopregnancy. Mating was confirmed the following morning with the presence of a vaginal plug, and this day was designated day 1 of pseudopregnancy. Pseudopregnancy was confirmed with daily vaginal smears to check for an arrested cycle.[34] Pseudopregnant rats were sacrificed using the same method as for pregnant animals. Uterine horns from 5 rats on day 6 of pseudopregnancy were collected for immunofluorescence and Western blotting.

### Ovariectomized Animals

Bilateral ovariectomy was performed on 20 rats under anesthesia with an intraperitoneal injection of xylazine (4 mg/kg; TROY laboratories Pty Ltd, Smithfield, NSW, Australia) and ketamine (75 mg/kg; Parnell Laboratories Australia Pty Ltd, Alexandria, NSW, Australia), after which animals were allowed to recover for 3 weeks. Progesterone (Sigma-Aldrich, St. Louis, MO, USA) and 17-β-estradiol (Sigma-Aldrich) were dissolved using benzyl alcohol (Sigma-Aldrich) and peanut oil (1:4 vol/vol; carrier) to achieve doses within the normal physiological range.[35-37] Rats were randomly assigned to the following treatment groups (5 rats per treatment) and were given a subcutaneous injection in the rump for 3 consecutive days: group 1 (Vehicle Control [VC]) injected with 0.1 mL of carrier only (benzyl alcohol and peanut oil); group 2 (Estrogen only [E]) injected with 0.1 mL of 17-β-estradiol (0.5 μg/day); group 3 (Progesterone only [P]) injected with 0.1 mL of progesterone (5 mg/day); and group 4 (Progesterone and Estrogen [PE]) injected with 0.1 mL of progesterone (5 mg/day) for 3 days and on the third day received an additional injection of 0.1 mL of 17-β-estradiol (0.5 μg). After the final injection, rats were left for 24 hours before sacrifice, and uterine horns were collected for immunofluorescence and Western blotting.

### Antibodies

The primary antibodies used were rabbit polyclonal nectin-3 immunoglobulin G (IgG) (sc-28637; Santa Cruz Biotechnology, Dallas, TX, USA); mouse monoclonal occludin IgG (33-1500;

Life Technologies Australia Pty Ltd, Mulgrave, VIC, Australia); mouse monoclonal anti-l Afadin IgG (ab90809; Abcam, Cambridge, UK); and mouse monoclonal anti-β-actin (A1978; Sigma-Aldrich). The isotype control antibodies used were rabbit serum IgG (I5006; Sigma-Aldrich), and mouse serum IgG (I5381; Sigma-Aldrich). The secondary antibodies used were Fluorescein (FITC)-AffiniPure goat anti-rabbit IgG (111-095-144; Jackson ImmunoResearch Laboratories Inc, West Grove, PA, USA), sheep anti-rabbit IgG conjugated to Cy3 (C2306; Sigma-Aldrich), Fluorescein (FITC)-AffiniPure goat anti-mouse IgG (115-095-166; Jackson ImmunoResearch Laboratories Inc), goat anti-rabbit polyclonal horseradish peroxidase (HRP)-linked IgG (P0448; Dako, Glostrup, Denmark), and sheep anti-mouse polyclonal HRP-linked IgG (NA931 V; Dako).

### Immunofluorescence and Colocalization

Uterine horns were cut into 5-mm blocks, embedded in OCT medium (Tissue Tek; Sakura Finetek, Torrence, CA, USA), and frozen in super-cooled isopentane (VWR International, Murarrie, QLD, Australia). Frozen sections, 7-µm thick, were cut using a Leica CM3050 cryostat (Leica, Heerbrugg, Switzerland) and air-dried on gelatin-chrome alum-coated slides. Sections were fixed in 100% acetone (nectin-3, nectin-3/occludin; Thermo Fisher Scientific, Scoresby, VIC, Australia) for 15 minutes and air-dried for 30 minutes or fixed in 4% paraformaldehyde (nectin-3/afadin, Sigma-Aldrich) for 10 minutes and washed in phosphate-buffered saline (PBS) for 5 minutes. All sections were then blocked using 1% bovine serum albumin (Sigma-Aldrich) in PBS for 30 minutes and probed with primary antibodies (nectin-3: 2 µg/mL; occludin: 2.5 µg/mL; and l-afadin: 2 µg/mL) or the respective isotype control antibodies at the same concentrations overnight at 4°C. Sections were washed in PBS (3 × 5 minutes) and incubated with secondary antibodies (anti-rabbit FITC: 5 µg/mL; anti-rabbit Cy3: 0.33 µg/mL; and anti-mouse FITC: 5 µg/mL) for 2 hours at room temperature and washed in PBS (3 × 5 minutes). Sections were mounted with 25 µL of Vectashield with diaminophenylindole (DAPI) medium (Vector Laboratories, Burlingame, CA, USA), coverslipped, and examined with the Zeiss Deconvolution microscope (Carl Zeiss Pty Ltd, Australasia, North Ryde, NSW, Australia) using the reflected light filters: DAPI (365, 395LP, and 420LP), CY3 (545/30, 570LP, and 610/75), and Alexa 488 (480/40, 505LP, and 535/50). Images were captured using a Zeiss AxioCam HRm digital monochrome charge-coupled device (CCD) camera (Carl Zeiss Pty Ltd) and analyzed using the Zeiss Efficient Navigation (ZEN) software (Carl Zeiss Pty Ltd).

### Isolation of UECs

Uterine horns were cut longitudinally, and the luminal epithelium removed by gentle scraping using sterile surgical blades as described previously.[22,38] Isolated epithelium was placed immediately in either cold lysis buffer (50 mmol/L Tris-HCl, 1 mmol/L EDTA, 150 mmol/L NaCl, 0.5% sodium dodecyl sulfate [SDS], 2.5% DOC, 5% polyoxyethylene nonyl phenol [Igepal], 1% protease inhibitor cocktail, and 10% PhosSTOP phosphatase inhibitor [Roche, Castle Hill, New South Wales, Australia]; Sigma-Aldrich) or cold IP lysis buffer (50 mmol/L Tris-HCl [pH 8.0], 150 mmol/L NaCl, 1% Igepal, 1% protease inhibitor cocktail [Sigma-Aldrich], and 10% PhosSTOP phosphatase inhibitor [Roche]). The cell suspension was homogenized using a 23-gauge needle and a 1-mL syringe (Livingstone International, Rosebury, NSW, Australia) and briefly centrifuged at 8000 g for 30 seconds. The supernatant was removed, and the protein concentrations of lysates were measured using a bicinchoninic acid protein assay (MicroBCA Protein assay kit; VWR International) and a CLARIOstar microplate reader (BMG LabTech, Ortenburg, Germany). Cell lysates were then either used immediately for IP or snap frozen for Western blotting.

### Co-IP

Prior to IP, primary antibodies (nectin-3: 3 µg; l-afadin: 1 µg; and occludin: 3 µg) or respective isotype control antibodies at the same concentrations were cross-linked to PureProteome Protein G magnetic beads (Merck Millipore, Bedford, MA, USA) using 13 µg/mL dimethyl pimelimidate (Sigma-Aldrich) per the Abcam protocol. Cell lysates (300-500 µg per IP reaction) were added to the cross-linked antibody/beads, diluted with IP lysis buffer to a total volume of 50 µL, and incubated for 3 hours at 4°C under constant rotation. Lysates were magnetically removed, and the beads were washed up to 10 times with 1% phosphate-buffered saline with Tween 20 . Immunoprecipitated proteins were separated from beads with native elution (l-afadin) by incubation with 20 µL 0.2 mol/L glycine (pH 2.5) for 2 minutes, followed by neutralization with 5 µL 1 mol/L Tris (pH 8.5) or denaturing elution (nectin-3 and occludin) by incubation with 25 µL of sample buffer (8% glycerol, 50 mmol/L Tris-HCl, pH 6.8, 1.6% SDS, 0.024% bromophenol blue, and 4% β-mercaptoethanol) at 95°C for 10 minutes. Native elutes were combined with sample buffer (8% glycerol, 50 mmol/L Tris-HCl, pH 6.8, 1.6% SDS, and 0.024% bromophenol blue), and all elutes were loaded onto 10% resolving acrylamide gels and subjected to SDS-polyacrylamide gel electrophoresis (PAGE) as detailed in Western blotting.

### Western Blotting

Protein (20 µg) was combined with sample buffer (8% glycerol, 50 mmol/L Tris-HCl, pH 6.8, 1.6% SDS, 0.024% bromophenol blue, and 4% β-mercaptoethanol), loaded (without boiling) onto a 12% resolving acrylamide gel, and separated using SDS-PAGE (200 V for 45 minutes). Proteins were transferred (100 V for 1 hour and 45 minutes) to Immobilon™ polyvinylidene fluoride (PVDF) membranes (Merck Millipore), blocked using filtered 5% skim milk powder in Tris-buffered saline-Tween 20 (TBST; 10 mmol/L Tris-HCl [pH 7.4], 150 mmol/L NaCl, and 0.05% Tween 20) for 1 hour at room temperature

with gentle agitation, and incubated with primary antibody (nectin-3: 0.4 μg/mL, l-afadin: 0.2 μg/mL; and occludin: 0.5 μg/mL) diluted in 1% skim milk in TBST overnight at 4°C on a rocking platform. Membranes were rinsed in TBST (3 × 10 minutes), incubated with 0.125 μg/mL secondary HRP-linked antibody, diluted in 1% skim milk powder in TBST for 2 hours at room temperature, with gentle agitation, and rinsed again in TBST (3 × 5 minutes). Protein bands were visualized using Immobilon™ Western HRP Substrate (Merck Millipore) and captured using a CCD camera and the Bio-Rad ChemiDoc MP system (Bio-Rad Laboratories, Hercules, CA, USA). Membranes were then incubated in stripping buffer (62.5 mmol/L Tris-HCl (pH 6.7), 2% SDS, and 100 mmol/L β-mercaptoethanol) at 60°C for 45 minutes and reprobed with either the IP partner antibodies to confirm protein–protein interaction or β-actin primary antibodies (1 μg/mL) to confirm equal loading of samples.

### *Densitometry and Statistical Analysis*

Band intensities for all blots were obtained using the Volume Analysis Tool from the Bio-Rad Image Lab 4.0 software (Bio-Rad Laboratories), and the protein band intensities were divided by β-actin band intensities to obtain normalized intensity values. Statistical analysis was performed on normalized intensities with GraphPad Prism 6 software (GraphPad Software, Inc., La Jolla, CA, USA). The effect of stage of pregnancy and the effect of hormone treatment on nectin-3 protein in isolated UECs were evaluated in separate tests using a single factor analysis of variance (ANOVA) with days of pregnancy (D1, D3, D6, and D7) and hormone treatments (VC, E, P, PE) as factors, respectively. The Tukey's honest significant difference HSD post hoc test was then applied when ANOVA yielded significance ($P < .05$) to determine which pairs of the means were significantly different. The effect of the blastocyst on nectin-3 protein in isolated UECs (D6 vs PSD6) was evaluated using the Student's $t$ test ($P < .05$ was considered significant). Bar graphs were constructed with the mean ± standard error of the mean for all data.

## Results

### *Nectin-3 Redistributes From the Basal Cell Surface to the Apical Tight Junction in UECs at the Time of Implantation*

To assess the presence of nectin-3 in the rat uterus during early pregnancy, immunofluorescence was used to localize nectin-3 protein on days 1 (time of fertilization), 3, 6 (time of implantation), 7, and 9 (postimplantation) of early pregnancy (Figure 1). On day 1 of pregnancy, nectin-3 was localized to the cytoplasm of UECs, with some aggregation of staining in the basal region of the cells (Figure 1A). On day 3, nectin-3 was distributed within the UEC cytoplasm (Figure 1B). On day 6, nectin-3 was localized to the apical cell junctions (Figure 1C). On day 7, nectin-3 retained an apical distribution (Figure 1D); however, the staining was also cytoplasmic, similar to that

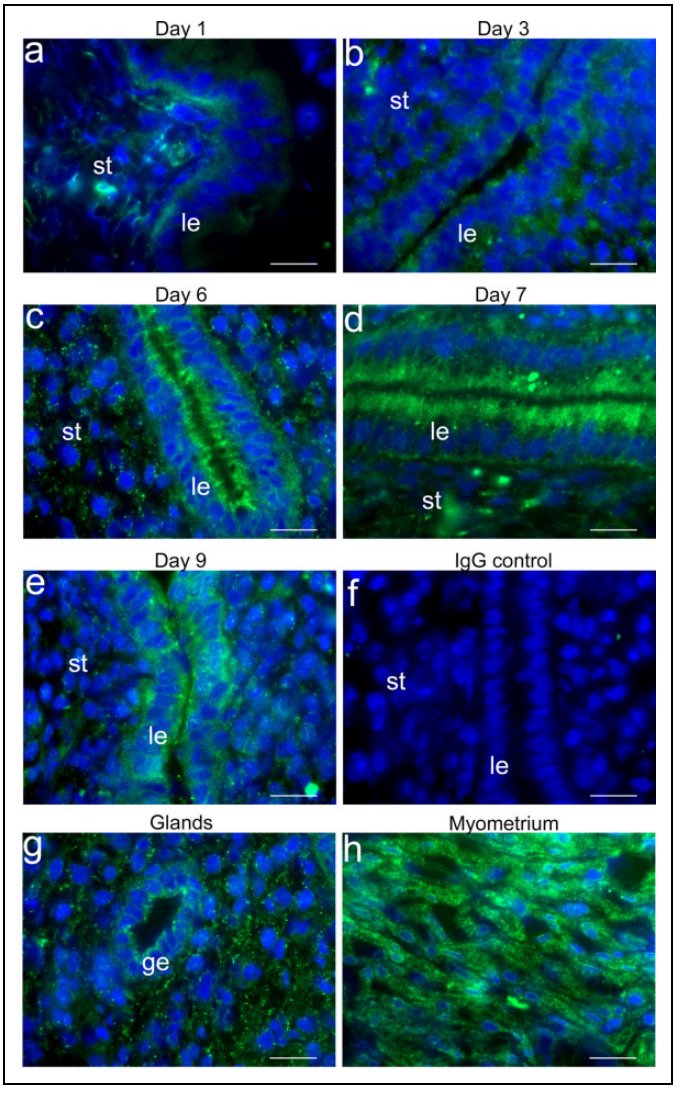


**Figure 1.** Nectin-3 protein localization in the rat uterus during days 1 to 9 of early pregnancy. Immunofluorescence micrographs showing nectin-3 protein (green, A488) and counterstained nuclei (blue, DAPI) in the uterine luminal epithelium in the endometrium on (A) day 1, (B) day 3, (C) day 6, (D) day 7, (E) day 9 of early pregnancy, with a representative (F) isotype (nonimmune) control of day 6 of pregnancy. Immunofluorescence micrographs showing nectin-3 protein (green, A488) and counterstained nuclei (blue, DAPI) in the (G) glandular epithelium of the endometrium and in the (H) smooth muscle cells of the myometrium, both on day 6 of pregnancy. All images are representative of staining obtained from 5 independent experiments. Scale bar 20 μm. DAPI indicates diaminophenylindole; ge, uterine glandular epithelium; le, uterine luminal epithelium; st, stroma. (The color version of this figure is available in the online version at http://rs.sagepub.com/.)

observed in day 6 pregnant animals. By day 9 of pregnancy, nectin-3 was again distributed throughout the cytoplasm of the UECs (Figure 1E).

Nectin-3 protein was also faintly distributed throughout the endometrial stroma (Figure 1A-E) in the cytoplasm of the glandular epithelium (Figure 1G) and the cytoplasm of the smooth muscle cells of the myometrium (Figure 1H); this

localization did not change between the sampled days of pregnancy. Isotype controls were performed alongside all experimental runs in this study; no staining was observed for any of the controls. A representative isotype control of rat uterus from day 6 of pregnancy is shown in Figure 1F.

## Nectin-3 Is Present in Uterine Epithelial Cells and Increases in Abundance at the Time of Implantation

Western blotting analysis of isolated UECs from rats on days 1, 3, 6, and 7 of pregnancy was used to measure the abundance of nectin-3 protein during early pregnancy. The results showed that nectin-3 was present in UECs as 3 molecular weight bands of 80, 60, and 32 kDa (Figure 2A). Densitometry and statistical analysis of the molecular weight protein band intensities for nectin-3 revealed a statistically significant increase in the total amount of nectin-3 ($P = .0419$, n = 5, Figure 2B) and specifically in the 60 kDa band ($P = .0142$, n = 5, Figure 2C) in UECs between day 1 of pregnancy (time of fertilization) and day 6 of pregnancy (time of implantation). There was also a statistically significant decrease in the amount of the 60 kDa band from day 6 of pregnancy to day 7 of pregnancy ($P = .0216$, n = 5, Figure 2C). The 32 kDa band also showed a statistically significant increase in the amount on day 7 of pregnancy compared to the other days of pregnancy (D1: $P = .0382$, D3: $P = .0272$, D6: $P = .0470$, n = 5, Figure 2D). The abundance of the 80 kDa band, however, did not change between the days of pregnancy sampled (ANOVA $P = .6746$, n = 5, Figure 2E). On day 6 of pregnancy, the 60 kDa band was also the dominant form (80 kDa: $P = .0006$, 32 kDa: $P = .0011$, n = 5, Figure 2F).

## Progesterone Regulates the Localization, but Not Abundance, of Nectin-3 Protein in UECs

The ovarian hormones estrogen and progesterone drive critical protein and cellular changes necessary for uterine receptivity in rats.[39] For this study, rats were ovariectomized, treated with progesterone and estradiol, and the isolated UECs subjected to immunofluorescence and Western blotting analysis to investigate whether these hormones when administered separately induce changes to nectin-3 protein localization and abundance. Ovariectomized rats treated with the minimal hormonal requirement (2 consecutive days of progesterone and combined progesterone and estrogen on the third day) to induce receptivity[39] were also analyzed to investigate whether changes to nectin-3 protein occur under these conditions.

Immunofluorescence analysis of uterine tissue taken from hormone-treated rats demonstrated differences in nectin-3 protein localization, suggesting that estrogen and progesterone can drive changes in nectin-3 localization (Figure 3). In vehicle-treated rats (VC), nectin-3 was distributed in the cytoplasm of UECs (Figure 3A). In rats subjected to estrogen treatment alone (E), nectin-3 was distinctly localized to the basal aspect of the cells with additional staining evident in the underlying stroma (Figure 3B), similar to that observed in rats on day 1 of pregnancy in Figure 1A. In rats treated with progesterone alone (P) and with the progesterone and estrogen in combination (PE), nectin-3 was localized to the apical cell junctions, with a similar pattern of staining to that observed for rats on day 6 of pregnancy in Figure 1C. No staining was observed in any of the isotype controls; a representative isotype control of rat uterus treated with progesterone is presented in Figure 3E.

Western blotting analysis of hormone-treated rats showed that nectin-3 presented as the same 3 molecular weight forms of the protein observed in normal pregnancy (Figure 3F). Densitometry and statistical analysis of the molecular weight isoforms revealed no statistically significant differences in either the total amount (ANOVA $P = .1922$, n = 5, Figure 3G) or the 60 kDa band (ANOVA $P = .1362$, n = 5, Figure 3H) of nectin-3 between the 4 treatment groups in the study. However, as in normal pregnancy, the 60 kDa band was the dominant protein band in rats treated with progesterone and estrogen (80 kDa: $P < .0001$; 32 kDa: $P < .0001$, n = 5, Figure 3I). There was also no statistically significant difference in the amounts of the 80 kDa (ANOVA $P = .5132$, n = 5, Figure 3J) or 32 kDa (ANOVA $P = .2987$, n = 5, Figure 3K) protein bands between the 4 treatment groups.

## The Blastocyst Does Not Increase the Abundance of Nectin-3 Protein at 60 kDa

As ovarian hormones were not responsible for inducing an increase in the abundance of the 60 kDa band of nectin-3, the study next used sterile mating to induce pseudopregnancy in female rats to determine whether pregnancy-specific factors and the presence of the blastocyst may be responsible for the increase in the levels of the 60 kDa band of nectin-3 (Figure 4). Immunofluorescence analysis of uterine tissue taken from day 6 pseudopregnant rats (Figure 4A) showed similar patterns of localization when compared to uteri from day 6 pregnant animals (Figure 4B). In both groups, nectin-3 localized to the apical junctions of UECs. Isotype controls were also performed, and no staining was observed in any of the control sections. A representative isotype control of rat uterus from day 6 of pseudopregnancy is shown in Figure 4C.

Western blotting analysis of isolated UECs from day 6 of pseudopregnant rats showed that nectin-3 was present as the 3 molecular weight bands obtained in day 6 of pregnant animals: 80 kDa, 60 kDa, and 32 kDa (Figure 4D). Densitometry and statistical analysis of both total nectin-3 protein ($P = .3565$, n = 5, Figure 4E) and the 60 kDa band ($P = .5010$, n = 5, Figure 4F) revealed no statistically significant difference between day 6 of pregnant and day 6 pseudopregnant animals, suggesting that the blastocyst does not affect the amount of nectin-3 protein in UECs around the time of implantation. The analysis of individual protein bands specifically on day 6 of pseudopregnancy, however, showed that there was a significantly greater amount of the 60 kDa band when compared to the 80 kDa band of nectin-3 protein ($P = .0073$, n = 5, Figure 4G). There was also no statistically significant difference in the amounts of the 80 kDa ($P = .2840$, n = 5, Figure 4H) or 32 kDa ($P = .2595$, n = 5, Figure 4I) protein bands between day 6 pregnant and day 6 pseudopregnant animals.

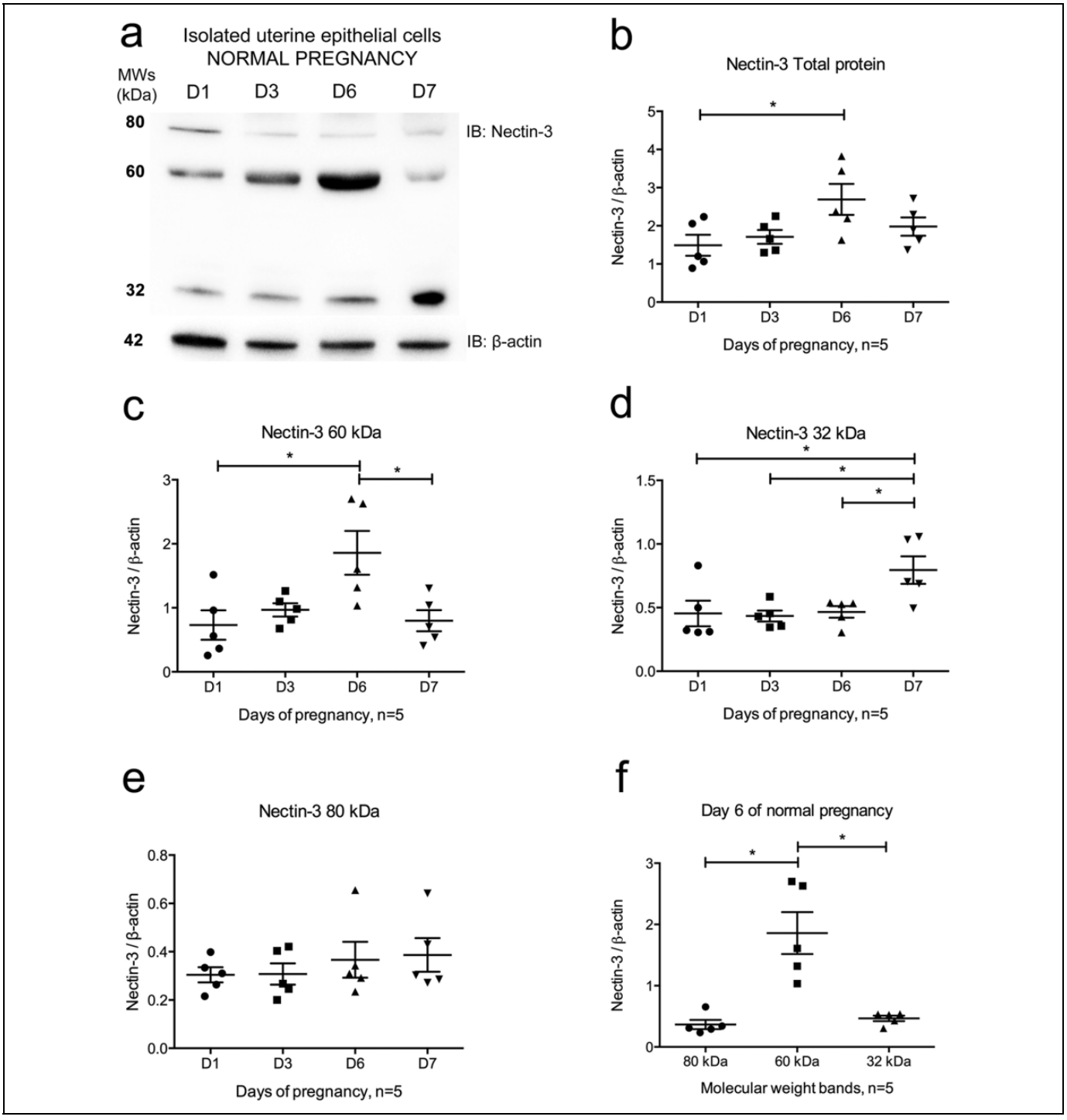


**Figure 2.** Nectin-3 protein abundance in isolated UECs during days 1 to 7 of early pregnancy. A, Western blotting image of nectin-3 protein from isolated UECs on day 1 (D1), day 3 (D3), day 6 (D6), and day 7 (D7) of pregnancy with β-actin as the loading control. Images are representative of immunoblotting obtained from 5 independent experiments. B-F, Scatter plots showing the normalized band intensity values and statistical analysis (1-way ANOVA and Tukey post hoc test) results for (B) total nectin-3 protein, (C) nectin-3 60 kDa, (D) nectin-3 32 kDa, (E) nectin-3 80 kDa during days 1 to 7 of normal pregnancy, and (F) nectin-3 molecular weight bands on day 6 of normal pregnancy. Each bar is the mean ± SEM, n = 5. Asterisks indicate statistical significance where $P < .05$. ANOVA indicates analysis of variance; IB, immunoblotting; MWs (kDa), molecular weights (kilodaltons); SEM, standard error of the mean; UECs, uterine luminal epithelial cells.

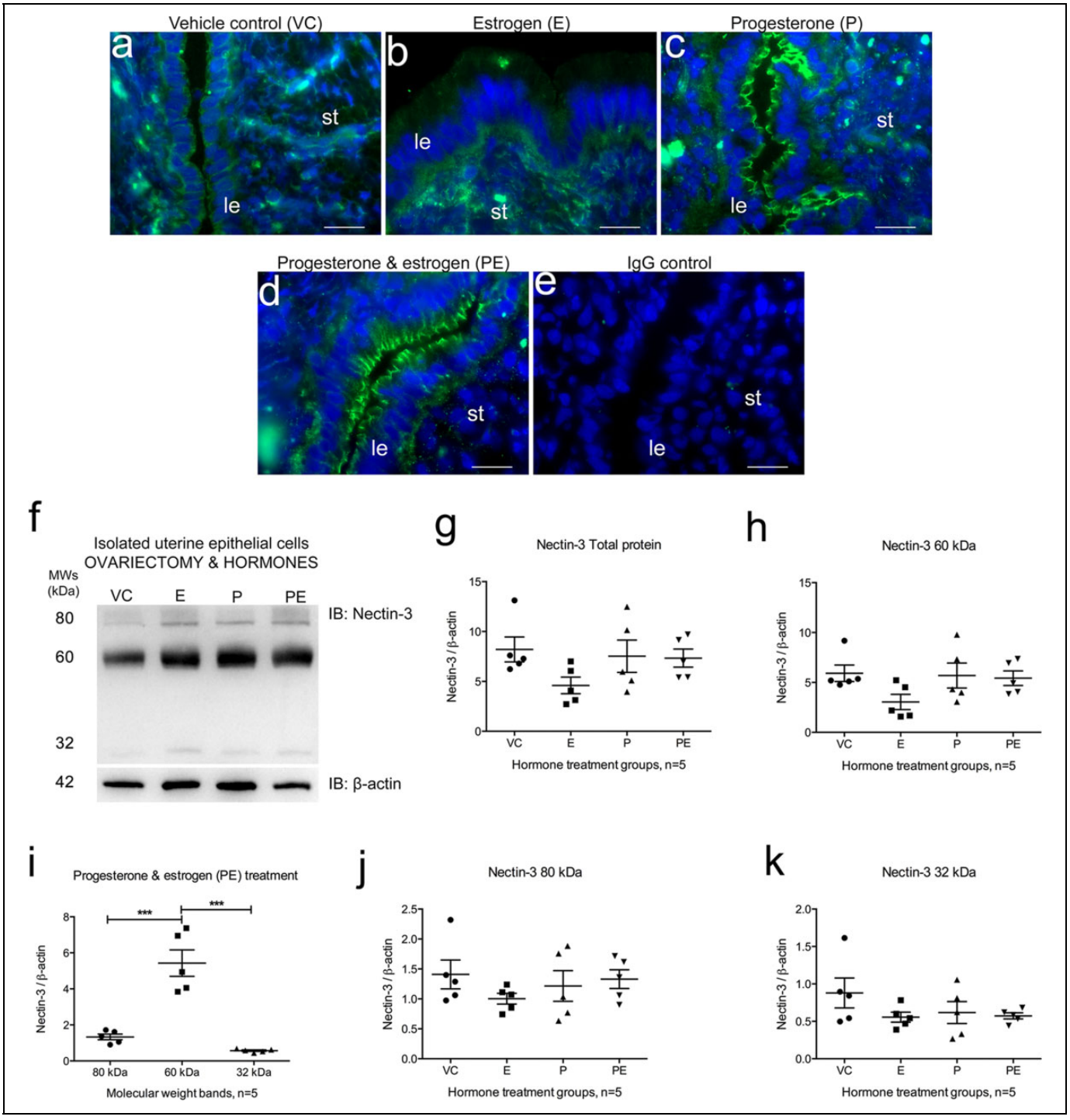


**Figure 3.** Nectin-3 protein localization (A-E) and abundance in UECs (F-I) of ovariectomized rats treated with hormones. Immunofluorescence micrographs of nectin-3 protein (green, A488) and counterstained nuclei (blue, DAPI) in UECs of ovariectomized rats treated with (A) vehicle only (VC), (B estrogen only (E), (C) progesterone only (P), and (D) progesterone and estrogen (PE). E, Isotype (nonimmune) control from a progesterone- and estrogen-treated rat. All images are representative of staining obtained from 5 independent experiments. Scale bar 20 μm. F, Western blotting image of nectin-3 protein in isolated UECs from rats treated with vehicle (VC), estrogen (E), progesterone (P), and progesterone and estrogen (PE). G-K, Scatter plots showing the normalized band intensity values and statistical analysis (1-way ANOVA and Tukey post hoc test) results for (G) total nectin-3 protein, (H) nectin-3 60 kDa, (I) nectin-3 molecular weight bands with progesterone and estrogen treatment, (J) nectin-3 80 kDa, and (K) nectin-3 32 kDa. Each bar is the mean ± SEM, n = 5. Asterisks indicate statistical significance where $P < .001$. ANOVA indicates analysis of variance; DAPI, diaminophenylindole; IB, immunoblotting; le, uterine luminal epithelium; MWs (kDa), molecular weights (kilodaltons); SEM, standard error of the mean; st, stroma; UECs, uterine luminal epithelial cells. (The color version of this figure is available in the online version at http://rs.sagepub.com/.)

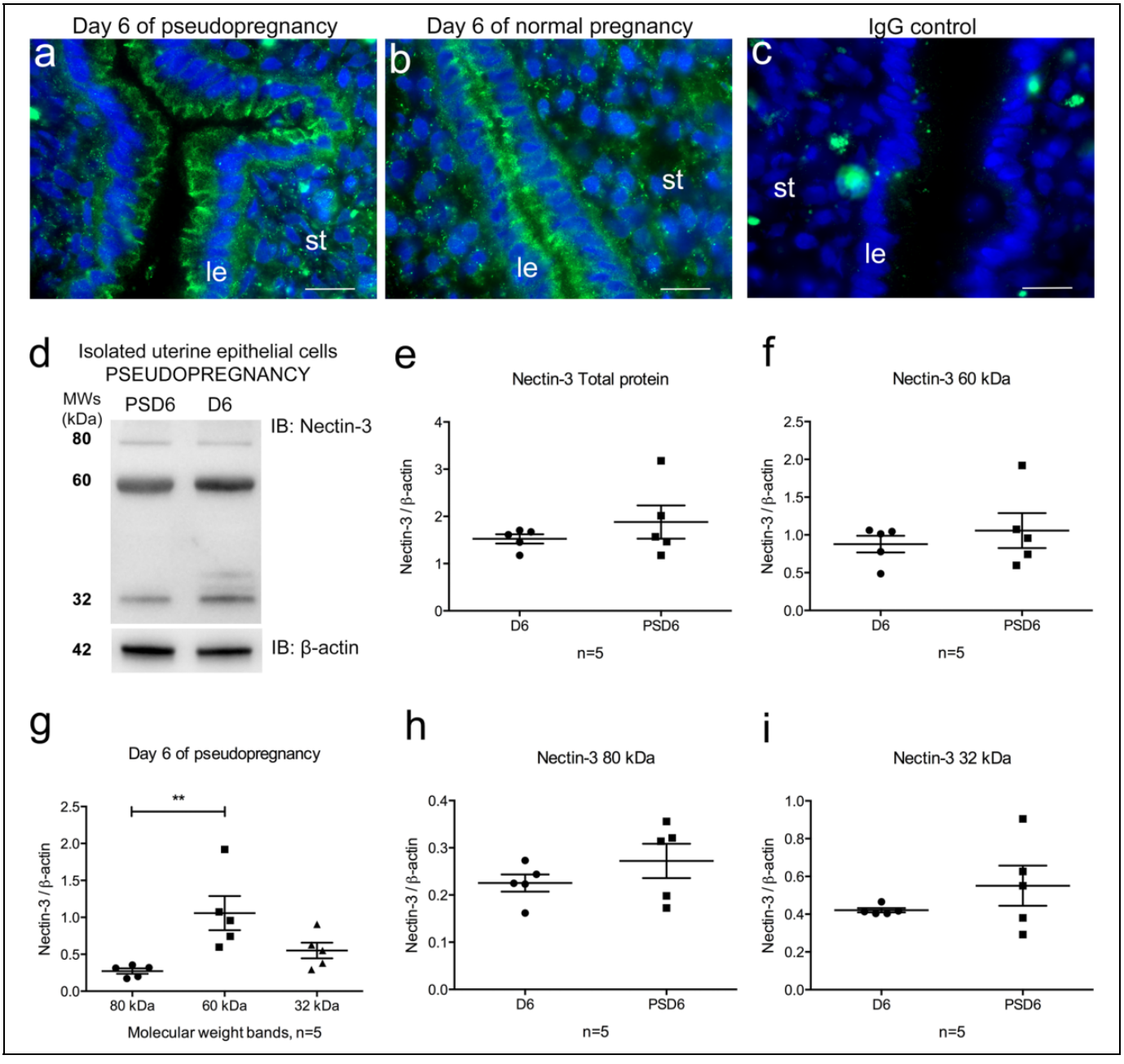


**Figure 4.** Nectin-3 protein localization (A-C) and abundance (D-G) in UECs from day 6 of pseudopregnancy compared to day 6 of normal pregnancy. Immunofluorescence micrographs of nectin-3 protein (green, A488) and counterstained nuclei (blue, DAPI) in UECs from day 6 of (A) pseudopregnancy and (B) normal pregnancy. C, Isotype (nonimmune) control from day 6 of pseudopregnancy. All images are representative of staining obtained from 5 independent experiments. Scale bar 20 μm. D, Western blotting image of nectin-3 protein on day 6 of pseudopregnancy (PSD6) and day 6 (D6) of normal pregnancy with β-actin as the loading control. Image is representative of immunoblotting obtained from 5 independent experiments. E-I, Scatter plots showing the normalized band intensity values and statistical analysis (Student *t* test, 1-way ANOVA, and Tukey post hoc test) results of (E) total nectin-3 and (F) nectin-3 60 kDa when comparing between day 6 of normal pregnancy and pseudopregnancy, (G) the 3 molecular weight bands of nectin-3 on day 6 of pseudopregnancy (H) nectin-3 80 kDa, and (I) nectin-3 32 kDa. Each bar is the mean ± SEM, n = 5. Asterisks indicate statistical significance where $P < .01$. ANOVA indicates analysis of variance; DAPI, diaminophenylindole; IB, immunoblotting; le, uterine luminal epithelium; MWs (kDa), molecular weights (kilodaltons); SEM, standard error of the mean; st, stroma; UECs, uterine luminal epithelial cells. (The color version of this figure is available in the online version at http://rs.sagepub.com/.)

Nectin-3 colocalizes with l-afadin and partially colocalizes with occludin but does not coimmunoprecipitate with protein in UECs at the time of implantation.

Given that nectin-3 appeared to localize to the apical cell junctions at this time, the study next investigated whether nectin-3 was involved in the tight junction through colocalization

and co-IP experiments with occludin. Occludin is a tight junction protein that is upregulated specifically at the time of implantation in UECs, when the tight junction is extended.[23] Colocalization immunofluorescence showed that nectin-3 colocalized with occludin in UECs at the time of implantation (Figure 5A-C); however, co-IP experiments showed that the 2 proteins do not coimmunoprecipitate (Figure 5E). Isotype controls were performed for both colocalization and co-IP analyses; no staining was observed in any of the controls (Figure 5D and E).

Nectin-3 has also been frequently linked to the actin cytoskeleton by l-afadin, an actin filament-binding protein.[40-42] Thus, this study next used colocalization and co-IP to investigate whether nectin-3 was linked to the actin cytoskeleton through l-afadin. Colocalization immunofluorescence showed that nectin-3 colocalized with l-afadin in UECs at the time of implantation (Figure 6A-C). Co-IP analysis (Figure 6E), however, showed that the 2 proteins do not interact. Isotype controls were performed for all immunofluorescence and IP reactions; no staining was observed in any of the controls (Figure 6D and E).

## Discussion

The AJC of the uterine luminal epithelium, comprising the tight junction, adherens junction and desmosomes, undergoes major modification in the transition to uterine receptivity in the rat.[8-10] This study sought to determine whether nectin-3, an intercellular adhesion protein frequently associated with the AJC in other epithelial tissues,[27] plays a similar role in the uterus. It was hypothesized that nectin-3 may be present at the intercellular junctions at the time of fertilization, a time when the AJC is intact.[9] The present study, however, showed results that contrast with the outlined hypothesis.

This study found that nectin-3 was present in the cytoplasm and at the basal surface of UECs as 3 molecular weights of 80 kDa, 60 kDa, and 32 kDa on day 1 of pregnancy at the time of fertilization, when UECs are not receptive to implantation. At the time of implantation (day 6 of pregnancy), the 60 kDa form of the protein increased with relocalization of the protein to the tight junction of UECs. After the implantation period, when UECs revert to a nonreceptive state,[1] nectin-3 decreased in abundance and redistributed back to the cell cytoplasm. This study is the first to document nectin-3 protein during early pregnancy in the rat. Nectin-3 has been found previously in the human endometrium,[32] where this protein was localized to the membrane of the glandular epithelium, however, no changes were observed between the proliferative and secretory phases of the menstrual cycle.

Nectin-3 is proposed to exist as 3 protein isoforms, α, β, and γ, with calculated molecular weights of 60 kDa, 55 kDa, and 47 kDa, respectively.[27] In the present study, only the 60 kDa protein band matches the calculated molecular weight of the α isoform, with the other 2 bands, 80 and 32 kDa, differing considerably from that previously reported for the β and γ isoforms. Nectin-3 has been reported previously in transfected Cos1 (monkey kidney) cells at 83 kDa[40]; however, as the protein undergoes a high level of *N*-glycosylation, as also observed for L cells (mouse cell line),[27] it is likely the 80 kDa band reported in this study may represent a cell-specific variation in the posttranslational glycosylation process. There

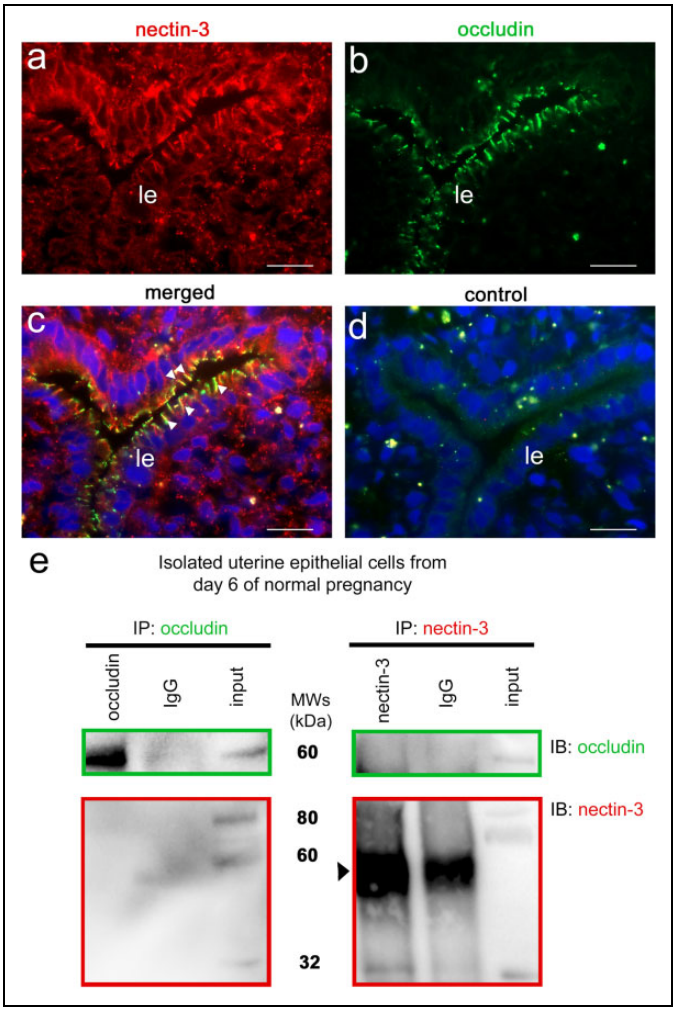


**Figure 5.** Nectin-3 colocalization (A-D) and coimmunoprecipitation (E) with occludin on day 6 of pregnancy. A-D, Immunofluorescence micrographs of nectin-3 and occludin colocalization experiments: (A) nectin-3 protein (single channel, red, Cy3), (B) occludin protein (single channel, green, Alexa 488), and (C) merged triple channel micrograph of nectin-3 protein (red, Cy3), occludin protein (green, Alexa 488) and counterstained nuclei (blue, DAPI). D, Merged triple channel micrograph of isotype (nonimmune) controls. Images are representative of staining obtained from 3 independent experiments. le, uterine luminal epithelium, arrows, areas of colocalization. Scale bar 20 μm. E, Western blotting images of coimmunoprecipitation (co-IP) assays performed on isolated UEC lysates from day 6 of pregnancy and using cross-linked nectin-3 and occludin antibodies. Images are representative of immunoprecipitation and immunoblotting obtained from 3 independent experiments. Arrow indicates heavy chain immunoglobulin dimer residue from immunoprecipitation reaction at ~50 kDa; DAPI, diaminophenylindole; IP, immunoprecipitation; IB, immunoblot; IgG, immunoglobulin control; input, IP lysate; MWs (kDa), Molecular Weights (kilodaltons); UEC, uterine luminal epithelial cell. (The color version of this figure is available in the online version at http://rs.sagepub.com/.)

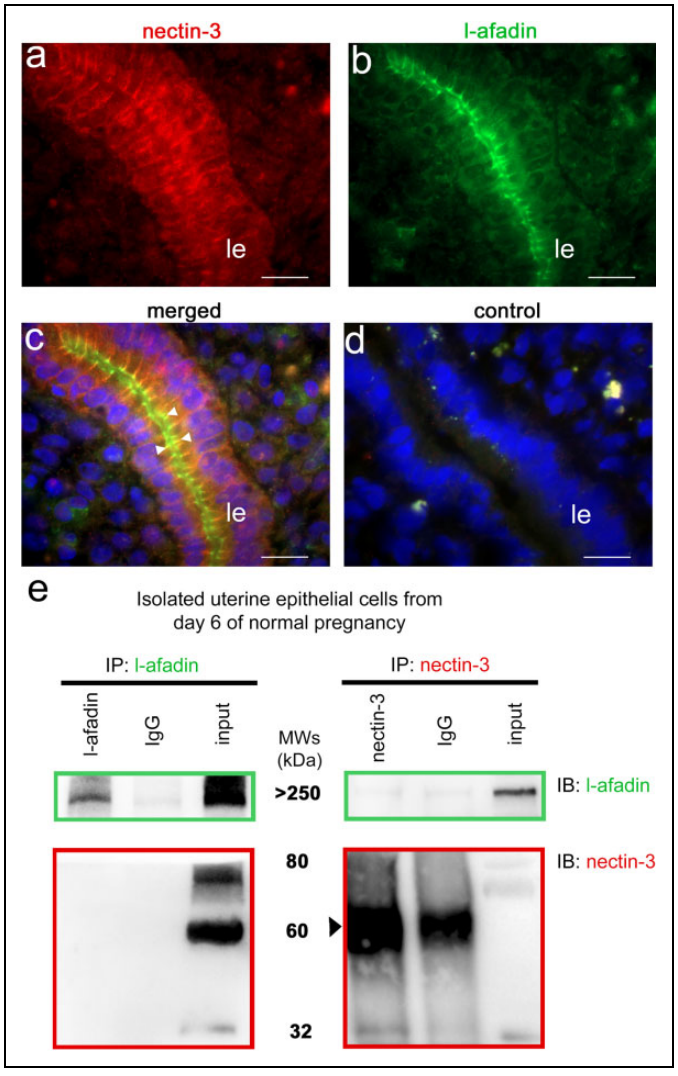


**Figure 6.** Nectin-3 colocalization (A-D) and coimmunoprecipitation (E) with l-afadin on day 6 of pregnancy. A-D, Immunofluorescence micrographs of nectin-3 and l-afadin colocalization experiments: (A) nectin-3 protein (single channel, red, Cy3), (B) l-afadin protein (single channel, green, Alexa 488), and (C) merged triple channel micrograph of nectin-3 protein (red, Cy3), l-afadin protein (green, Alexa 488) and counterstained nuclei (blue, DAPI). D, Merged triple channel micrograph of isotype (nonimmune) controls. Images are representative of staining obtained from 3 independent experiments. Scale bar 20 μm. E, Western blotting images of coimmunoprecipitation (co-IP) assays performed on isolated UEC lysates from day 6 of pregnancy and using cross-linked nectin-3 and l-afadin antibodies. Images are representative of immunoprecipitation and immunoblotting obtained from 3 independent experiments. Arrow indicates heavy chain immunoglobulin dimer residue from immunoprecipitation reaction at ~50 kDa; arrows, areas of colocalization, DAPI, diaminophenylindole; IP, immunoprecipitation; IB, immunoblot; IgG, immunoglobulin control; input, IP lysate; le, uterine luminal epithelium; MWs (kDa), molecular weights (kilodaltons); UEC, uterine luminal epithelial cell. (The color version of this figure is available in the online version at http://rs.sagepub.com/.)

also have been no previous reports of the 32 kDa, but as nectin-3 is susceptible to cleavage by the enzyme γ-secretase,[43] the 32 kDa may represent another processing variant of the protein.

The relocation of nectin-3 from the basal cell surface to the cellular junction specifically at the time of implantation is a particularly interesting finding. Nectin-3 is frequently associated with the junctional complex in various epithelial tissues,[27,44] where it serves to mediate the initial adhesive forces to recruit first E-cadherin for the formation of the adherens junction and then claudins and occludins to establish the apical tight junction,[29,41] completing the junctional complex. A similar but altered mechanism may operate in the uterus as E-cadherin,[25] claudin-1,[23] and occludin[23] also localize to the apico-lateral borders of UECs at the time of implantation.

However, in the present study, nectin-3 was localized to the cellular junctions, specifically at the time of implantation, when the adherens junction is lost.[9] This result is unusual, as nectin-3 is understood to predominantly localize to the adherens junction, where it mediates adhesion and provides the stimulating signals to initiate tight junction formation.[29,45] Thus far, there have been no reports involving nectin-3 in the regulation of paracellular permeability as is well documented for claudins[46] and occludin,[47] key facilitators of this function in the tight junction.[48] Therefore, it may be that the localization of nectin-3 to the cellular junctions may represent a compensatory mechanism to maintain adhesion and retain some epithelial barrier integrity given the loss of the adherens junction and desmosomes in UECs at this time.

The hypothesis that nectin-3 may support compensatory intercellular adhesion may further be supported with the increase in the 60 kDa α-isoform of the nectin-3 protein specifically at the time of implantation. The α-isoform of nectin-3 is documented to be the main variant that mediates adhesion in L cells (mouse cell line)[27] and thus, an increase in the abundance of this isoform coincident with localization to the tight junction provides a strong connection for this adhesive function.

This study also showed that localization of nectin-3 to the cellular junctions requires ovarian progesterone; however, ovarian hormones alone were not sufficient to increase the levels of the 60 kDa α-isoform in UECs. Furthermore, it was observed that there was no significant difference in the amount of this isoform between pregnant and pseudopregnant rats on day 6 of pregnancy. These results indicate that neither ovarian hormones nor the blastocyst are responsible for the protein increase, but taken further, that other factors common to the pregnant and pseudopregnant state may be causing this change. One potential candidate is seminal plasma, which has been observed to augment progesterone levels.[49] Since progesterone was able to induce localization changes in nectin-3, it may be that exposure to seminal plasma may be required to increase levels of ovarian progesterone that are sufficient to induce a concomitant increase in the levels of the 60 kDa α-isoform of nectin-3.

The final set of results in this study also demonstrated that while nectin-3 colocalized with both occludin and l-afadin, nectin-3 did not coimmunoprecipitate with the proteins, indicating that nectin-3 does not directly interact with occludin or l-afadin at the time of implantation. Nectin-3 has been reported to colocalize with occludin at the tight junction in previous studies, however, the association has usually been transient and

at a time prior to the establishment of a stable junctional complex in motile cells.[50] The indication that nectin-3 does not associate with l-afadin in UECs, however, remains a unique observation, given that the two proteins are well documented in a variety of cell types to together mediate a separate adhesion complex, alongside the E-cadherin/β-catenin/α-catenin complex within the adherens junction.[51,52] Thus, the present results pose an interesting and unique situation in which nectin-3 and l-afadin colocalize in the same junctional region, but do not appear to interact. Given that UECs dismantle many of their adhesions mediating intercellular attachment, and the adherens junction is lost at the time of implantation,[9] it may be that an independent nectin-3 complex is required to mediate some intercellular adhesion to maintain the tight junction but also mediate adhesion that is sufficiently weak to be breached by the embryo during the attachment process.

Another possibility is that nectin-3 may also interact with the other isoform of the afadin protein, s-afadin, which has been documented previously.[40,53] S-afadin was originally believed to be restricted to brain tissues; however, recently other tissues have been reported to produce the s-afadin protein.[42] Thus far, there have been no reports on the presence of afadin in uterine tissues, and therefore a nectin-3/s-afadin interaction remains to be investigated in UECs.

In summary, this study showed that nectin-3 was present in the rat endometrium as 3 protein isoforms and increased at the cellular junctions of UECs, specifically at the time of implantation. It also appears that progesterone is responsible for the localization of nectin-3 at the cellular junctions, however, the factor responsible for increasing the abundance of the 60 kDa protein isoform remains to be identified. The presence of nectin-3 at the cellular junction may serve to maintain intercellular adhesion as compensation for loss of the adherens junction and desmosomes, and thus maintain some element of mucosal integrity at this critical time.

## Acknowledgments

The authors would like to acknowledge Dr Louise Cole (Core Facilities Manager, Bosch Institute Advanced Microscopy Facility, The University of Sydney) for her assistance with the microscopy imaging (Zeiss Deconvolution and Zeiss LSM 510 Metaconfocal microscopes) and Dr Donna Lai (Molecular Biology Officer, Bosch Institute Molecular Biology Facility, The University of Sydney) for her support with Western blotting.

## Declaration of Conflicting Interests

The author(s) declared no potential conflicts of interest with respect to the research, authorship, and/or publication of this article.

## Funding

The author(s) disclosed receipt of the following financial support for the research, authorship, and/or publication of this article: This work was supported by the Australian Research Council, the NWG Macintosh Memorial Fund, the Elizabeth and Henry Hamilton-Browne scholarship, and by funds from the Murphy laboratory.

## References

1. Murphy CR. Uterine receptivity and the plasma membrane transformation. *Cell Res*. 2004;14(4):259-267.
2. Finn CA, Martin L. The control of implantation. *Reproduction*. 1974;39(1):195-206.
3. Wang Q, Margolis B. Apical junctional complexes and cell polarity. *Kidney Int*. 2007;72(12):1448-1458. doi:10.1038/sj.ki.5002579.
4. Farquhar MG. Junctional complexes in various epithelia. *J Cell Biol*. 1963;17(2):375-412. doi:10.1083/jcb.17.2.375.
5. Furuse M. Molecular Basis of the Core Structure of Tight Junctions. *Cold Spring Harbor Perspectives in Biology*. 2010;2(1):a002907. doi:10.1101/cshperspect.a002907.
6. Tsukita S, Furuse M, Itoh M. Multifunctional strands in tight junctions. *Nat Rev Mol Cell Biol*. 2001;2(4):285-293. doi:10.1038/35067088.
7. Hartsock A, Nelson WJ. Adherens and tight junctions: structure, function and connections to the actin cytoskeleton. *Biochim Biophys Acta*. 2008;1778(3):660-669. doi:10.1016/j.bbamem.2007.07.012.
8. Murphy CR, Swift JG, Mukherjee TM, Rogers AW. The structure of tight junctions between uterine luminal epithelial cells at different stages of pregnancy in the rat. *Cell Tissue Res*. 1982;223(2):281-286.
9. Murphy CR. Junctional barrier complexes undergo major alterations during the plasma membrane transformation of uterine epithelial cells. *Hum Reprod*. 2000;15(suppl 3):182-188.
10. Preston AM, Lindsay LA, Murphy CR. Desmosomes in uterine epithelial cells decrease at the time of implantation: an ultrastructural and morphometric study. *J Morphol*. 2006;267(1):103-108.
11. Albaghdadi AJH, Kan FWK. Endometrial receptivity defects and impaired implantation in diabetic NOD mice. *Biol Reprod*. 2012;87(2):30.
12. Ghosh D, Danielson KG, Alston JT, Heyner S. Functional differentiation of mouse uterine epithelial cells grown on collagen gels or reconstituted basement membranes. *In Vitro Cell Dev Biol*. 1991;27A(9):713-719.
13. Illingworth IM, Kiszka I, Bagley S, Ireland GW, Garrod DR, Kimber SJ. Desmosomes are reduced in the mouse uterine luminal epithelium during the preimplantation period of pregnancy: a mechanism for facilitation of implantation. *Biol Reprod*. 2000;63(6):1764-1773.
14. Johnson SA, Morgan G, Wooding FB. Alterations in uterine epithelial tight junction structure during the oestrous cycle and implantation in the pig. *J Reprod Fertil*. 1988;83(2):915-922.
15. Bowen JA, Newton GR, Weise DW, Bazer FW, Burghardt RC. Characterization of a polarized porcine uterine epithelial model system. *Biol Reprod*. 1996;55(3):613-619.
16. Mani SK, Decker GL, Glasser SR. Hormonal responsiveness by immature rabbit uterine epithelial cells polarized in vitro. *Endocrinology*. 1991;128(3):1563-1573.
17. Winterhager E, Kühnel W. Alterations in intercellular junctions of the uterine epithelium during the preimplantation phase in the rabbit. *Cell Tissue Res*. 1982;224(3):517-526.

18. Winterhager E, Mendoza AS. Structure of quick-frozen tight junctions in uterine epithelium of pseudopregnant rabbits. *Z Mikrosk Anat Forsch*. 1987;101(1):179-185.
19. Murphy CR, Swift JG, Need JA, Mukherjee TM, Rogers AW. A freeze-fracture electron microscopic study of tight junctions of epithelial cells in the human uterus. *Anat Embryol (Berl)*. 1982; 163(4):367-370. doi:10.1007/BF00305552.
20. Murphy CR, Rogers PA, Hosie MJ, Leeton J, Beaton L. Tight junctions of human uterine epithelial cells change during the menstrual cycle: a morphometric study. *Acta Anat (Basel)*. 1992;144(1):36-38.
21. Someya M, Kojima T, Ogawa M, et al. Regulation of tight junctions by sex hormones in normal human endometrial epithelial cells and uterus cancer cell line Sawano. *Cell Tissue Res*. 2013;354(2):481-494. doi:10.1007/s00441-013-1676-9.
22. Nicholson MDO, Lindsay LA, Murphy CR. Ovarian hormones control the changing expression of claudins and occludin in rat uterine epithelial cells during early pregnancy. *Acta Histochem*. 2010;112(1):42-52.
23. Orchard MD, Murphy CR. Alterations in tight junction molecules of uterine epithelial cells during early pregnancy in the rat. *Acta Histochem*. 2002;104(2):149-155.
24. Hyland RA, Shaw TJ, Png FY, Murphy CR. Pan-cadherin concentrates apically in uterine epithelial cells during uterine closure in the rat. *Acta Histochem*. 1998;100(1):75-81.
25. Slater M, Murphy CR, Barden JA. Tenascin, E-cadherin and P2X calcium channel receptor expression is increased during rat blastocyst implantation. *Histochem J*. 2002;34(1-2): 13-19.
26. Preston AM, Lindsay LA, Murphy CR. Progesterone treatment and the progress of early pregnancy reduce desmoglein 1&2 staining along the lateral plasma membrane in rat uterine epithelial cells. *Acta Histochem*. 2003;106(5):345-351.
27. Satoh-Horikawa KK, Nakanishi HH, Takahashi KK, et al. Nectin-3, a new member of immunoglobulin-like cell adhesion molecules that shows homophilic and heterophilic cell-cell adhesion activities. *J Biol Chem*. 2000;275(14): 10291-10299.
28. Takai Y. Nectin and afadin: novel organizers of intercellular junctions. *J Cell Sci*. 2003;116(1):17-27.
29. Kuramitsu K, Ikeda W, Inoue N, Tamaru Y, Takai Y. Novel role of nectin: implication in the co-localization of JAM-A and claudin-1 at the same cell-cell adhesion membrane domain. *Genes Cells*. 2008;13(8):797-805.
30. Takai YY, Ikeda WW, Ogita HH, Rikitake YY. The immunoglobulin-like cell adhesion molecule nectin and its associated protein afadin. *Cell Dev Biol*. 2007;24:309-342.
31. Inagaki M, Irie K, Ishizaki H, Tanaka-Okamoto M, Miyoshi J, Takai Y. Role of cell adhesion molecule nectin-3 in spermatid development. *Genes Cells*. 2006;11(9):1125-1132. doi:10.1111/j.1365-2443.2006.01006.x.
32. Ballester M, Gonin J, Rodenas A, et al. Eutopic endometrium and peritoneal, ovarian and colorectal endometriotic tissues express a different profile of Nectin-1, -3, -4 and nectin-like molecule 2. *Hum Reprod*. 2012;27(11):3179-3186.
33. Okabe N, Ozaki-Kuroda K, Nakanishi H, Shimizu K, Takai Y. Expression patterns of nectins and afadin during epithelial remodeling in the mouse embryo. *Dev Dyn*. 2004;230(1): 174-186.
34. Swingle WW, Seay P, Perlmutt J, Collins EJ, George Barlow JR, Fedor EJ. An experimental study of pseudopregnancy in rat. *Am J Physiol—Leg Content*. 1951;167(3):586-592.
35. Ljungkvist I.Attachment reaction of rat uterine luminal epithelium. II. The effect of progesterone on the morphology of the uterine glands and the luminal epithelium of the spayed, virgin rat. *Acta Soc Med Ups*. 1971;76(3-4):110-126.
36. Ljungkvist I.Attachment reaction of rat uterine luminal epithelium. 3. The effect of estradiol, estrone and estriol on the morphology of the luminal epithelium of the spayed, virgin rat. *Acta Soc Med Ups*. 1971;76(3-4):139-157.
37. Murphy CR, Rogers AW. Effects of ovarian hormones on cell membranes in the rat uterus. III. The surface carbohydrates at the apex of the luminal epithelium. *Cell Biophys*. 1981;3(4):305-320.
38. Kaneko YY, Lindsay LALA, Murphy CRCR. Focal adhesions disassemble during early pregnancy in rat uterine epithelial cells. *Reprod Fertil Dev*. 2008;20(8):892-899.
39. Psychoyos A. Hormonal control of ovoimplantation. *Vitam Horm*. 1973;31:201-256.
40. Reymond N, Borg JP, Lecocq E, et al. Human nectin3/PRR3: a novel member of the PVR/PRR/nectin family that interacts with afadin. *Gene*. 2000;255(2):347-355.
41. Takai Y, Irie K, Shimizu K, Sakisaka T, Ikeda W. Nectins and nectin-like molecules: Roles in cell adhesion, migration, and polarization. *Cancer Sci*. 2003;94(8):655-667.
42. Tanaka-Okamoto M, Hori K, Ishizaki H, et al. Involvement of afadin in barrier function and homeostasis of mouse intestinal epithelia. *J Cell Sci*. 2011;124(pt 13):2231-2240.
43. Kim J, Chang A, Dudak A, Federoff HJ, Lim ST. Characterization of nectin processing mediated by presenilin-dependent γ-secretase. *J Neurochem*. 2011;119(5):945-956.
44. Mizoguchi A, Nakanishi H, Kimura K, et al. Nectin: an adhesion molecule involved in formation of synapses. *J Cell Biol*. 2002; 156(3):555-565.
45. Yamada T, Kuramitsu K, Rikitsu E, Kurita S, Ikeda W, Takai Y. Nectin and junctional adhesion molecule are critical cell adhesion molecules for the apico-basal alignment of adherens and tight junctions in epithelial cells. *Genes Cells*. 2013;18(11):985-998.
46. Krause G, Winkler L, Mueller SL, Haseloff RF. Structure and function of claudins. *Biochim Biophys Acta*. 2008;1778(3): 631-645.
47. Cummins PM. Occludin: one protein, many forms. *Mol Cell Biol*. 2012;32(2):242-250.
48. Anderson JM, Van Itallie CM. Physiology and function of the tight junction. *Cold Spring Harb Perspect Biol*. 2009;1(2): a002584.
49. O'Leary S, Jasper MJ, Robertson SA, Armstrong DT. Seminal plasma regulates ovarian progesterone production, leukocyte recruitment and follicular cell responses in the pig. *Reproduction*. 2006;132(1):147-158.
50. Martin TA, Lane J, Harrison GM, Jiang WG. The expression of the Nectin complex in human breast cancer and the role of Nectin-

3 in the control of tight junctions during metastasis. *PLoS One*. 2013;8(12):e82696. doi:10.1371/journal.pone.0082696.

51. Takahashi K.Nectin/PRR: An immunoglobulin-like cell adhesion molecule recruited to cadherin-based adherens junctions through interaction with afadin, a PDZ domain-containing protein. *J Cell Biol*. 1999;145(3):539-549.
52. Mandai K, Rikitake Y, Shimono Y, Takai Y. Afadin/AF-6 and canoe: roles in cell adhesion and beyond. *Prog Mol Biol Transl Sci*. 2013;116:433-454.
53. Kobayashi R, Kurita S, Miyata M, et al. s-Afadin binds more preferentially to the cell adhesion molecules nectins than l-afadin. *Genes to Cells*. 2014;19(12):853-863. doi:10.1111/gtc.12185.